



Cite this: *RSC Adv.*, 2017, 7, 47366

# Co–N–C supported on SiO<sub>2</sub>: a facile, efficient catalyst for aerobic oxidation of amines to imines†

Chenghui Zhang,<sup>a</sup> Pengshan Zhao,<sup>a</sup> Zongliang Zhang,<sup>b</sup> Jingwei Zhang,<sup>a</sup> Ping Yang,<sup>a</sup> Peng Gao,<sup>b</sup> Jun Gao<sup>id</sup><sup>a</sup> and Di Liu<sup>id</sup><sup>\*a</sup>

We developed a novel, facile preparation method of Co–N–C/SiO<sub>2</sub>, which was the pyrolysis of silicone gel containing metal ion and triethanolamine (TEA) prepared by sol–gel process. N<sub>2</sub> adsorption–desorption characterization displayed the sample had high specific surface area and pore volume (220.9 m<sup>2</sup> g<sup>−1</sup>, 0.67 mL g<sup>−1</sup>). The active Co appeared to be small particles with size of about 5 nm and was well dispersed on SiO<sub>2</sub>. And the highly dispersed cobalt and nitrogen-doped carbon in Co–N–C/SiO<sub>2</sub> served as active phase for the oxidation of amines to imines, thus Co–N–C/SiO<sub>2</sub> could efficiently catalyze the oxidation of amines to imines in solvent-free, air atmospheric conditions, avoiding the use of large excesses of additives, specialized oxidant and solvent.

Received 28th August 2017  
 Accepted 3rd October 2017

DOI: 10.1039/c7ra09516c

rsc.li/rsc-advances

## Introduction

Imines are a class of reactive nitrogen-containing compounds which are widely utilized in aziridination, reduction, cyclization, condensation and addition reactions.<sup>1</sup> The traditional preparation of imines by the condensation of aldehydes or ketones with primary amines cannot meet the requirements of green chemistry,<sup>2</sup> great efforts have been made to develop more facile and green synthetic strategies.<sup>3</sup> The oxidation coupling of amines to imines as a effective method has been developed.<sup>4</sup> Traditionally, noble-metal complexes (*e.g.*, Ru-, Au-, Pd-) were widely used for the oxidation of amines to imines. Although these complexes exhibited good yields and selectivity,<sup>5</sup> they had disadvantages of high cost and poor reusability. In order to overcome these drawbacks, some supported noble-metal catalysts were employed to achieve this transformation,<sup>6</sup> but harsh reaction conditions were usually required, and the cost of such noble-metal catalysts was still unacceptable. In addition, Cu-<sup>7</sup> and Fe<sup>8</sup>-based catalysts, bioinspired catalysis,<sup>9</sup> photocatalysis<sup>10</sup> and mesoporous carbon<sup>11</sup> were developed. These catalytic systems showed varying degrees of success as well as limitations like laborious work-up procedures, use of oxidant and/or toxic organic solvents. Therefore, research of efficient catalyst system for the oxidation of amines is desirable.

Recently, N-doped carbon base metal-based catalysts (M–N–C, M = Co, Fe, Ni) were found to be effective for a variety of organic redox transformations.<sup>12</sup> According to the current study,

the preparation of M–N–C materials was mainly by the pyrolysis of metal–organic framework (MOF)<sup>13</sup> and the complex of metal component–nitrogen compounds (phenanthroline, melamine, *etc.*) supported on carbon nanotubes, CMK-3, *etc.*<sup>14</sup> Obviously, these methods were not suitable for large-scale preparation due to the use of expensive and fabricating complex materials.

Here, we developed a N-doped carbon based metal supported by SiO<sub>2</sub> material, which is easily obtained by the pyrolysis of silicone gel containing metal ion and triethanolamine (TEA) prepared by sol–gel process, and the material has low cost without the use of expensive materials. In this work, the M–N–C/SiO<sub>2</sub> was employed to catalyze aerobic oxidation of amines to imines, and the catalytic performance, applicability and reusability of the catalyst were investigated in detail.

## Results and discussion

Initially, the self-oxidative coupling reaction of benzylamine was selected as the test reaction to optimize of the reaction conditions. We firstly investigated four N-doped carbon based transition metal catalysts, which exhibited from poor to moderate catalytic properties (Table 1, entries 1–4). Co–N–C possessed the best catalytic performance among the M–N–C screened. In order to further improve the activity of Co–N–C, Co–N–C supported by SiO<sub>2</sub> (8.8 wt% load of Co) was prepared to catalyze the model reaction under the same condition and gave imine in 92% yield (Table 1, entries 5). Meanwhile, Co–N–C/SiO<sub>2</sub> catalysts with 5 wt% and 15 wt% load of Co were investigated. Unfortunately, they did not exhibit higher activity (Table 1, entries 6–7). The pyrolysis temperature also affected the catalytic efficiency of Co–N–C/SiO<sub>2</sub>. The activity of Co–N–C/SiO<sub>2</sub> pyrolyzed at 500 °C significantly decreased, and the yield of the expected product did not further increased when the pyrolysis

<sup>a</sup>College of Chemical and Environmental Engineering, Shandong University of Science and Technology, Qingdao, 266590, P. R. China. E-mail: ld002037132@163.com

<sup>b</sup>State Key Laboratory of Bioactive Seaweed Substances, Qingdao Brightmoon Seaweed Group Co Ltd, Qingdao, 266400, P. R. China

† Electronic supplementary information (ESI) available: IR, <sup>1</sup>H NMR, <sup>13</sup>C NMR and MS spectral data for compounds. See DOI: 10.1039/c7ra09516c



Table 1 Optimization of the reaction conditions<sup>a</sup>

1a  $\xrightarrow[110^\circ\text{C}]{\text{air, catalyst}}$  3a

Entry	Catalysts	Conditions	Pyrolysis temperature (°C)	Yield <sup>b</sup> [%]
1	Cu–N–C	8.8 wt% Cu/6 mol%/solvent-free	600	40
2	Ni–N–C	8.8 wt% Ni/6 mol%/solvent-free	600	34
3	Fe–N–C	8.8 wt% Fe/6 mol%/solvent-free	600	35
4	Co–N–C	8.8 wt% Co/6 mol%/solvent-free	600	57
5	Co–N–C/SiO <sub>2</sub>	8.8 wt% Co/6 mol%/solvent-free	600	92
6	Co–N–C/SiO <sub>2</sub>	5 wt% Co/6 mol%/solvent-free	600	81
7	Co–N–C/SiO <sub>2</sub>	15 wt% Co/6 mol%/solvent-free	600	70
8	Co–N–C/SiO <sub>2</sub>	8.8 wt% Co/6 mol%/solvent-free	500	78
9	Co–N–C/SiO <sub>2</sub>	8.8 wt% Co/6 mol%/solvent-free	700	92
10 <sup>c</sup>	N–C/SiO <sub>2</sub>	Solvent-free	600	68
11	Co–N–C/SiO <sub>2</sub>	8.8 wt% Co/8 mol%/solvent-free	600	99
12	Co–N–C/SiO <sub>2</sub>	8.8 wt% Co/8 mol%/ethanol	600	27
13	Co–N–C/SiO <sub>2</sub>	8.8 wt% Co/8 mol%/toluene	600	34
14	Co–N–C/SiO <sub>2</sub>	8.8 wt% Co/8 mol%/DMF	600	70

<sup>a</sup> Reaction conditions: amine (10 mmol), catalyst (amount of catalyst was calculated based on metal), 110 °C, 24 h, 1 atm air. <sup>b</sup> Yield of isolated product. <sup>c</sup> Amount of N–C/SiO<sub>2</sub>: 0.424 g.

temperature rose from 600 °C to 700 °C (Table 1, entries 5, 8–9). Thus, 600 °C should be a reasonable choice. The above results demonstrated the introduction of SiO<sub>2</sub> could greatly improve catalytic performance of Co–N–C. To clarify the mechanism of Co–N–C/SiO<sub>2</sub> with high activity, the catalysts were characterized and analyzed.

Firstly, elemental compositions of Co–N–C and Co–N–C/SiO<sub>2</sub> were determined, it could be seen from Table 2 that the main components were Co, C, N in the Co–N–C catalyst and Co, C, N, Si, O in the Co–N–C/SiO<sub>2</sub> catalyst. Also hydrogen was also detected in small quantities. XRD pattern of the Co–N–C (Fig. 1b) showed five diffraction peaks. Two weak reflections appeared around 26° and 43° attributed to characteristic of the graphitic-type lattice.<sup>15</sup> The other three diffraction peaks at around 44.2°, 51.6°, and 76.0° could be assigned to the (111), (200) and (220) planes of metallic Co<sup>0</sup> (PDF 15-0806), while only a weak and wide characteristic peak of metallic Co in XRD pattern of the Co–N–C/SiO<sub>2</sub> could be detected at around 44.2°, except for a broad halo peak around 22° ascribed to the (111) reflection of the SiO<sub>2</sub> lattice (PDF 76-0931) in Fig. 1a. XRD analysis manifested that the Co<sup>0</sup> phase was produced in the

pyrolysis for both Co–N–C and Co–N–C/SiO<sub>2</sub>. The size of cobalt particle calculated from the broadening of the Co (111) plane using the Scherrer equation is 3.28 nm, which signified Co<sup>0</sup> in the Co–N–C/SiO<sub>2</sub> was highly dispersed. This was further corroborated by TEM. Two fringes spacing of 0.205 nm corresponding to the (111) plane of Co<sup>0</sup> in HRTEM image of Co–N–C/SiO<sub>2</sub> were observed (Fig. 2b, inset),<sup>16</sup> the Co<sup>0</sup> appeared to be fine particles with size of about 5 nm and was well dispersed on the surface of silica (small dark dots in Fig. 2b). And the cobalt phase in Co–N–C was present in larger, non-uniform and concentrated state (Fig. 2a). Obviously, support-SiO<sub>2</sub> was helpful to hinder the Co nanoparticles growth.

Table 2 Analysis of catalyst composition<sup>a</sup>

Catalysts	H%	C%	N%	O%	Co%	Si%
Co–N–C	0.45	54.83	5.79	0.56	36.45	nd <sup>b</sup>
Co–N–C/SiO <sub>2</sub>	0.54	23.06	4.22	31.62	9.79	28.57

<sup>a</sup> The elements of C, N and H were determined by using CHNS elemental analyzer and the elements of Co was determined by using X-ray fluorescence spectrometer (XRF). <sup>b</sup> nd = not detected.

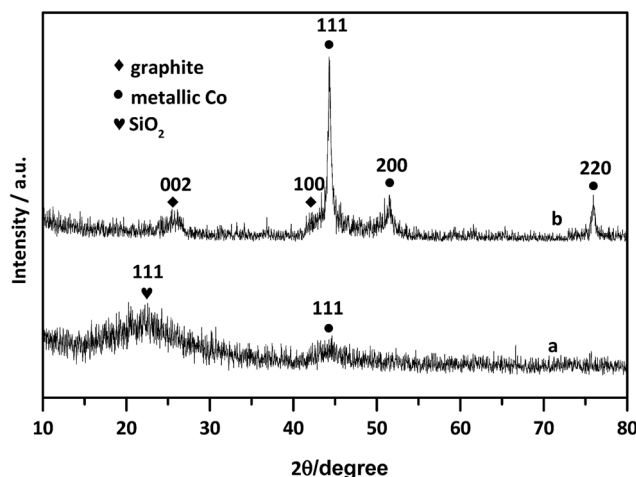


Fig. 1 XRD patterns of the as-prepared (a) Co–N–C/SiO<sub>2</sub>, (b) Co–N–C.



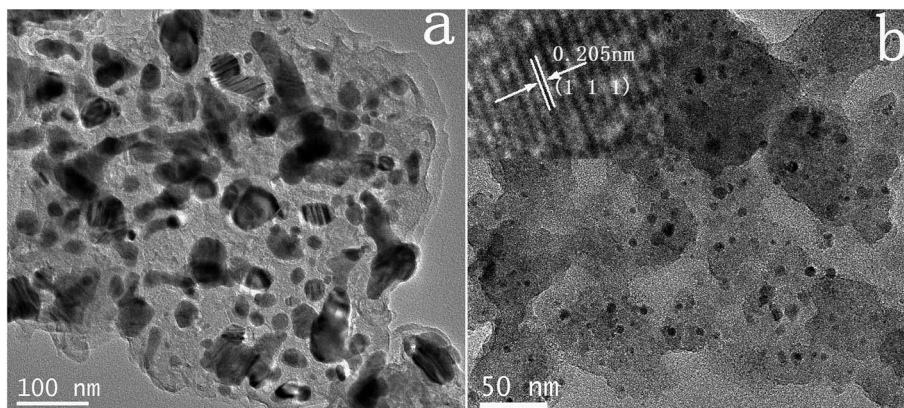


Fig. 2 TEM images of (a) Co-N-C and (b) Co-N-C/SiO<sub>2</sub>.

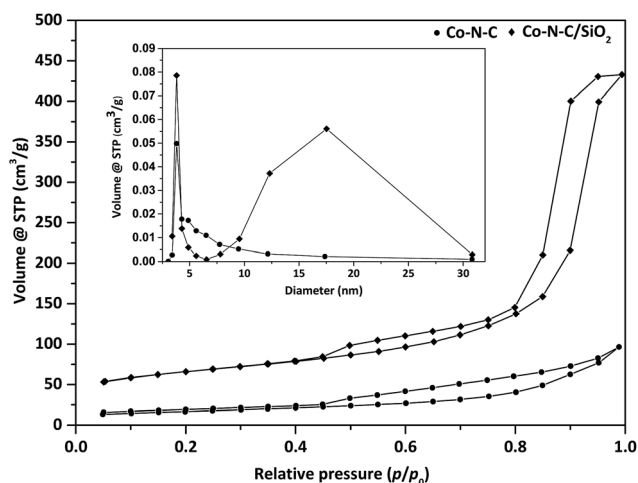


Fig. 3 N<sub>2</sub> adsorption-desorption isotherms and pore size distribution of Co-N-C and Co-N-C/SiO<sub>2</sub>.

Table 3 The textural properties of Co-N-C and Co-N-C/SiO<sub>2</sub> catalysts

Sample	$S_{\text{BET}}$ (m <sup>2</sup> g <sup>-1</sup> )	Pore volume (mL g <sup>-1</sup> )	Pore size (nm)
Co-N-C	58.1	0.15	3.82
Co-N-C/SiO <sub>2</sub>	220.9	0.67	3.81/17.53

Moreover, textural properties of Co-N-C and Co-N-C/SiO<sub>2</sub> were analyzed by N<sub>2</sub> adsorption-desorption isotherms (Fig. 3). A type IV adsorption isotherm followed by a well-developed hysteresis loop was observed for Co-N-C/SiO<sub>2</sub>, suggesting the mesoporous structure. The specific surface area and pore volume of Co-N-C/SiO<sub>2</sub> calculated by BET method were 220.9 m<sup>2</sup> g<sup>-1</sup> and 0.67 mL g<sup>-1</sup>, respectively (Table 3). The pore size distribution estimated by applying BJH method presented double pore distribution (3.81 nm, 17.53 nm) (Fig. 3, inset). Nevertheless, Co-N-C exhibited a type IV-like sorption isotherm with a poor hysteresis loop. The specific surface area and pore volume were much smaller than that of Co-N-C/SiO<sub>2</sub>. These analyses showed that the support SiO<sub>2</sub> facilitated the formation of developed porous organization. Apparently, the developed porous organization was beneficial to the exposure of more catalytic active sites, and promoted the catalytic activity accordingly.

Subsequently, XPS was performed to acquire more details on Co-N-C/SiO<sub>2</sub> catalyst structure. As shown in Fig. 4a, the peaks around 793.2 and 778.4 eV were ascribed to Co<sup>0</sup>,<sup>15</sup> while those around 786.3, 783.3 and 781.5 eV were in accordance with Co<sup>2+</sup> phase, which demonstrated Co<sup>2+</sup> was not thoroughly reduced in the pyrolysis. And the N 1s spectrum could be deconvoluted into four peaks, including graphitic N (400.7 eV), pyrrolic N (399.6 eV), pyridinic N (398.8 eV), and pyridinic N (398.3 eV) (Fig. 4b).<sup>11,17,18</sup>

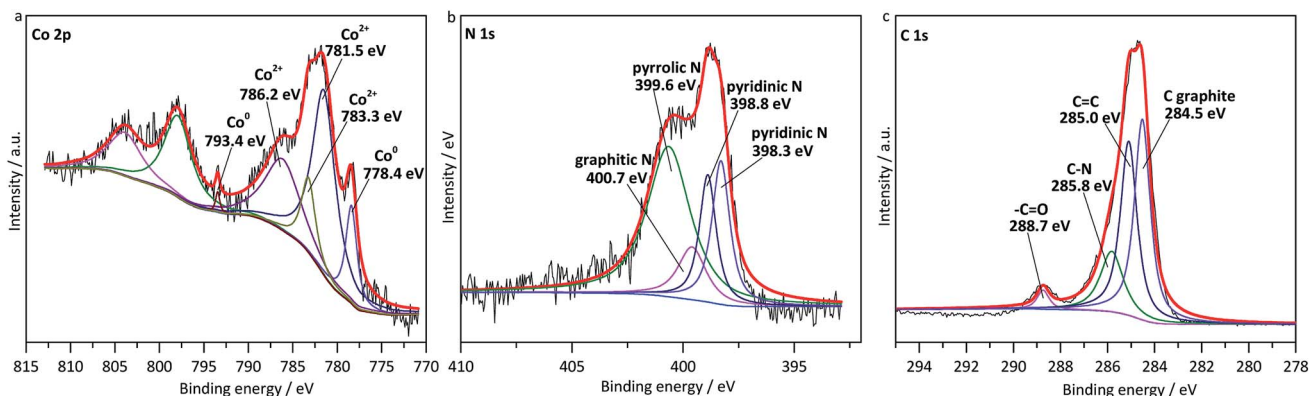
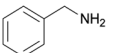
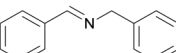
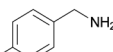
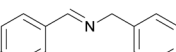
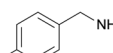
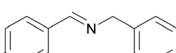
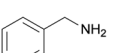
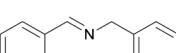
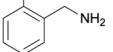
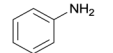
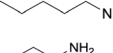
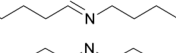
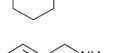
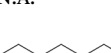
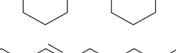
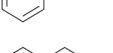
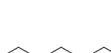
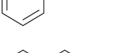
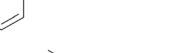
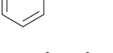
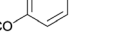
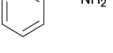
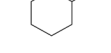
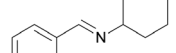


Fig. 4 XPS spectra of the Co 2p (a), N 1s (b), and C 1s (c).



Table 4 Aerobic photocatalytic oxidation of various amines over Co-N-C/SiO<sub>2</sub><sup>a</sup>

Entry	Substrate 1	Substrate 2	Molar ratio <sup>be</sup>	Time (h)	Reaction		Conversion <sup>cf</sup> (%)	Selectivity <sup>d</sup> (%)
					$R^1-NH_2$ 1	$H_2N-R^2$ 2		
					$R^1-NH_2 + H_2N-R^2 \xrightarrow[air, 110^\circ C]{8mol\% Co-N-C/SiO_2} R^1-CH=N-R^2$			
1		N.A.	N.A.	24		3a	99	100
2		N.A.	N.A.	26		3b	96	100
3		N.A.	N.A.	28		3c	97	100
4		N.A.	N.A.	30		3e	95	100
5		N.A.	N.A.	30		3d	93	100
6		N.A.	N.A.	24	nd	3h	nd	nd
7		N.A.	N.A.	24		3f	32	28
8		N.A.	N.A.	24		3g	13	62
9			1/1	24		3i	69	38
10			1/1.5	24		3i	76	69
11			1/3	24		3i	100	82
12			1/3	24		3j	100	89
13			1/3	24		3k	100	93
14			1/3	24		3l	100	35

<sup>a</sup> Reaction conditions: benzylamine and other aromatic and aliphatic amines (10 mmol), Co-N-C/SiO<sub>2</sub> (8 mol%), air, 110 °C. <sup>b</sup> Molar ratio of benzylamine and different amines. <sup>c</sup> Conversion was calculated based on substrate 1. <sup>d</sup> Selectivity was calculated based on products 3. <sup>e</sup> N.A. = no available. <sup>f</sup> nd = not detected.

In addition, the C 1s spectrum was fitted with four peaks centered at 288.7, 285.8, 285.0, and 284.5 eV (Fig. 4c), corresponding to the -C=O, N-C, C=C, and C graphite.<sup>19</sup> This was a powerful evidence that carbon was successfully doped with nitrogen. Previous studies have shown that carbon material doped with nitrogen was able to activate the oxygen molecules and substrates in oxidation reactions,<sup>20</sup> and our test also confirmed imine was produced with the yield of 68% over

metal-free N-C/SiO<sub>2</sub> (Table 1, entry 10), which manifested N-C possessed catalytic activity. In sum, the highly dispersed cobalt and nitrogen-doped carbon supported by SiO<sub>2</sub> served as active phase for oxidation of amines to imines, they played superimposing effect in the catalytic oxidation system, which seemed to explain why Co-N-C/SiO<sub>2</sub> possessed high catalytic activity.



Table 5 Recyclability of the Co–N–C/SiO<sub>2</sub> catalyst<sup>a</sup>

Run	1	2	3	4	5
Yield <sup>b</sup> (%)	98	98	95	94	95

<sup>a</sup> Reaction conditions: amine (10 mmol), catalyst (8 mol%), amount of catalyst was calculated based on metal, 110 °C, 24 h, air. <sup>b</sup> Yield of isolated product.

After obtaining the optimized catalyst, the effect of the catalyst dosage was investigated. When the catalyst dosage increased from 6 mol% to 8 mol%, there was an improvement (92% vs. 99%) in the reaction yield (Table 1, entry 5 and 11). And an 8% mol amount of Co–N–C/SiO<sub>2</sub> was sufficient to promote the reaction. Also the reaction was studied catalyzed by Co–N–C/SiO<sub>2</sub> (8 mol%) using different solvents (Table 1, entries 12–14). The results displayed the best yield was obtained under solvent-free conditions although the desired products could be formed in solvents. Therefore, we decided to carry out the subsequent reactions of the amines in the amount of 8 mol% Co–N–C/SiO<sub>2</sub> under solvent-free conditions. Apparently, this catalytic system was very simple because no special atmosphere and additives were required compared with other metal-catalyzed reactions.<sup>21</sup>

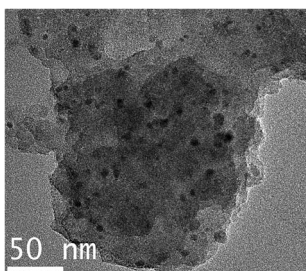
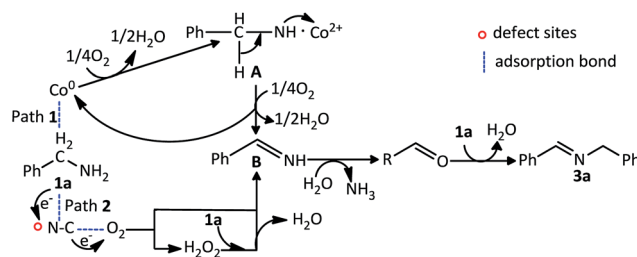
With this optimized procedure in hand, the applicability of the heterogeneous Co–N–C/SiO<sub>2</sub> catalyst for the oxidation self-coupling of amines was studied using various combinations of substrates (Table 4). Benzylic amines gave the imines as the main product with high conversion and high selectivity after different times, and all ring-substituted benzylamines coupled at a slower rate than benzyl amine. Functional groups such as methyl (Table 4, entry 2), halogens (Table 4, entries 3–5) were shown to be highly applicable to the present reaction conditions. Electron donating (Table 4, entry 2) and electron-withdrawing substituents (Table 4, entries 3–5) smoothly proceeded. The reactivity of the regioisomer decreased in the order of *para* > *meta* > *ortho* isomer, which indicated the presence of a steric effect. However, no reaction occurred for the oxidation of aniline lacking a hydrogen atom under the same condition (Table 4, entry 6). In addition, a primary aliphatic amine was also converted to the corresponding coupled imine, but the conversion and selectivity were lower than those of benzylic homologues (Table 4, entries 7–8).

Next, we focused on examining the oxidation cross-coupling of amines over the same catalytic system. Reactions between benzylamine and *n*-hexylamine were firstly performed, a low

selectivity of unsymmetric imine (38%) was observed at the molar ratio of hexylamine to benzylamine of 1 : 1 (Table 4, entry 9). Increasing the molar ratio of hexylamine to benzylamine could remarkably improve the selectivity to the unsymmetric imine. Good selectivity for quantitative conversion of benzylamine was achieved when the molar ratio of hexylamine to benzylamine is 3 : 1 (Table 4, entry 11). Then, the oxidation cross-coupling of structurally different amines were investigated with this ratio. The tested aliphatic amines gave the corresponding unsymmetric imines in high selectivity (Table 4, entries 12, 13), while the very low selectivity (35%) of unsymmetrical imine for the reaction between benzylamine and aniline was obtained (Table 4, entry 14). These data of activity test demonstrated that cross-coupling of amines could produce the corresponding imines, but an excess of reagent was required, which meant the condensation of amines was not an efficient way for the preparation of cross-coupled imines.

Moreover, the recyclability of Co–N–C/SiO<sub>2</sub> was checked by separating the catalyst from the reaction mixture by simple filtration (Table 5). The Co–N–C/SiO<sub>2</sub> was washed with ethanol by sonication for two times, then reduced by H<sub>2</sub> flow at 400 °C for 2 h prior to reuse as the catalyst in the next run. The Co–N–C/SiO<sub>2</sub> catalyst could be used repeatedly 5 cycles for amine oxidation without any significant loss of the activity (98–94%), indicating the excellent stability of the Co–N–C/SiO<sub>2</sub> catalyst. Further, we performed TEM characterization for the spent catalyst after 1 cycle to investigate the Co particle size distribution, showing no significant change was observed compared to fresh catalyst (Fig. 2b vs. Fig. 5).

Furthermore, a plausible reaction mechanism for the oxidation coupling of amines to imines is shown in Scheme 1. Firstly, water was detected in the reaction medium by GC-MS. And the above studies have found that Co and N–C in the Co–N–C/SiO<sub>2</sub> have catalytic activity for the aerobic oxidation of amines, respectively. Based on these facts and previous literature reports,<sup>2a,22</sup> two pathways are proposed in terms of different active phase, (1) Co as active phase: a dehydration reaction of the benzylamine occurs in the presence of oxidized Co to form the complex A. Then, A is further oxidized leading to benzylimine B, meanwhile the cobalt is regenerated in this step; (2) N–C as active phase: both benzylamine and molecular oxygen are activated on the defect sites of N–C and subsequently transform into benzylimine and H<sub>2</sub>O<sub>2</sub> intermediates. H<sub>2</sub>O<sub>2</sub> can react immediately with another molecular 1a to obtain

Fig. 5 TEM image of spent Co–N–C/SiO<sub>2</sub> catalyst.Scheme 1 Proposed mechanism for the aerobic oxidation of amines to imines over Co–N–C/SiO<sub>2</sub>.

benzylimine B. These two pathways proceed *via* oxidative dehydrogenation of the amine to benzylimine B. As aldehyde in reaction mixture was observed, we believe the intermediate B reacts with H<sub>2</sub>O generated in the initial step to give the aldehyde C with liberation of ammonia, subsequently a dehydration–condensation reaction of the aldehyde with reactant amine occurs to obtain the final product 3a.

## Conclusions

In this paper, a novel, simple preparation strategy of Co–N–C/SiO<sub>2</sub> catalyst was developed. The obtained catalyst benefits from the use of safe and inexpensive starting materials, and exhibits high catalytic activity for oxidation coupling of amines to imines under mild reaction conditions. More work is under way to further explore its potential application in the field of oxidative esterification of alcohols and dehydrogenative coupling of alcohols with amines.

## Experimental

### Preparation

Preparation step of the catalyst as follows:

(1) Preparation of silicone gel including Co and triethanolamine: to a water solution containing Co(NO<sub>3</sub>)<sub>2</sub>·6H<sub>2</sub>O (1.79 g, 6.15 mmol) and nitric acid (2 mL) were added with vigorous stirring. Then, triethanolamine (TEA, 2.80 g, 18.77 mmol) and tetraethyl orthosilicate (TMOS, 8 mL) were added dropwise to the solution. After the solution became homogeneous, addition of a spot of NH<sub>4</sub>F caused gelation at room temperature, giving a uniform and stable gel.

(2) Pyrolysis of silicone gel: before pyrolysis, a precursor was obtained by drying the silicone gel at 80 °C for 12 h. Then the precursor was heated to 600 °C at a rate of 3 °C min<sup>−1</sup> in highly pure N<sub>2</sub> and held at the final temperature for 2 h in tube furnace, followed by naturally cooling to room temperature to obtain the catalyst.

As a comparison, metal-free N–C/SiO<sub>2</sub> was also prepared by the same method. Unsupported M–N–C catalysts were obtained by pyrolysis of metal–TEA complex.

### Characterization

Powder X-ray diffraction patterns of the catalysts were recorded on a Rigaku diffractometer (Ultima IV, 3 kW) by Cu K $\alpha$  radiation (40 kV, 30 mA, 0.1543 nm). The size and morphology of the catalysts samples was determined by using a Transmission Electron Microscope (TEM, JEOL, JEM-1400Plus). The determination of elements of the catalysts samples was determined by using CHNS elemental analyzer (VARIO EL III) X-ray fluorescence spectrometer (XRF, AXIOS-Petro, 4 kW) and X-ray photoelectron spectroscopy (XPS, ESCALAB 250Xi, 150 W).

### Synthesis of 3a as a representative example

In a typical amine oxidation reaction, a mixture of benzylamine (1a; 10 mmol), Co–N–C/SiO<sub>2</sub> (0.482 g) was added in a 50 mL round bottom flask equipped with a condenser. The reaction

mixture was heated to 110 °C under vigorous stirring for specific time under an air atmosphere. After reaction, the mixture was cooled to 80 °C, 20 mL of ethanol was added to the mixture which was vigorously stirred to completely dissolution of product, and the catalyst was removed by filtration. The filtrate was determined by Shimadzu GC-2000 Plus and Agilent GC-MS 7890 to obtain characteristic and yield of product. The solvent evaporated under reduced pressure to gain crude product which was purified by silica gel flash chromatography using petroleum ether and ethyl acetate as eluent to afford the product.

## Conflicts of interest

There are no conflicts to declare.

## Acknowledgements

This work was supported by grants from Open Foundation of the State Key Laboratory of Bioactive Seaweed Substances, Qingdao Brightmoon Seaweed Group Co Ltd (No. SKL-BASS1723).

## Notes and references

- (a) S. Kobayashi and H. Ishitani, *Chem. Rev.*, 1999, **99**, 1069–1094; (b) J. P. Adams, *J. Chem. Soc., Perkin Trans. 1*, 2000, **1**, 125–139; (c) D. Chen, Y. Wang and J. Klankermayer, *Angew. Chem., Int. Ed.*, 2010, **49**, 9475–9478; (d) S. Kobayashi, Y. Mori, J. S. Fossey and M. M. Salter, *Chem. Rev.*, 2011, **111**, 2626–2704; (e) R. He, X. Jin, H. Chen, Z.-T. Huang, Q.-Y. Zheng and C. Wang, *J. Am. Chem. Soc.*, 2014, **136**, 6558–6561; (f) M. Kondo, N. Kobayashi, T. Hatanaka, Y. Funahashi and S. Nakamura, *Chem.–Eur. J.*, 2015, **21**, 9066–9070.
- (a) R. D. Patil and S. Adimurthy, *Asian J. Org. Chem.*, 2013, **2**, 726–744; (b) R. J. Angelici, *Catal. Sci. Technol.*, 2013, **3**, 279–296; (c) W. Qin, S. Long, M. Panunzio and S. Biondi, *Molecules*, 2013, **18**, 12264–12289; (d) B. L. Ryland and S. S. Stahl, *Angew. Chem., Int. Ed.*, 2014, **53**, 8824–8838.
- (a) B. Gnanaprakasam, J. Zhang and D. Milstein, *Angew. Chem., Int. Ed.*, 2010, **49**, 1468–1471; (b) M. A. Esteruelas, N. Honeczek, M. Olivan, E. Onate and M. Valencia, *Organometallics*, 2011, **30**, 2468–2471; (c) R. Cano, D. J. Ramon and M. J. Yus, *J. Org. Chem.*, 2011, **76**, 5547–5557; (d) A. Maggi and R. Madsen, *Organometallics*, 2012, **31**, 451–455; (e) G. Zhang and S. K. Hanson, *Org. Lett.*, 2013, **15**, 650–653.
- X. Lang, H. Ji, C. Chen, W. Ma and J. Zhao, *Angew. Chem., Int. Ed.*, 2011, **50**, 3934–3937.
- (a) L. He, T. Chen, D. Gong, Z. Lai and K. Huang, *Organometallics*, 2012, **31**, 5208–5211; (b) B. Zhu, M. Lazar, B. G. Trewyn and J. Robert, *J. Catal.*, 2008, **260**, 1–6; (c) X. Jin, Y. Liu, Q. Lu, D. Yang, J. Sun, S. Qin, J. Zhang, J. Shen, C. Chu and R. Liu, *Org. Biomol. Chem.*, 2013, **11**, 3776–3780.
- (a) M. S. Kwon, S. Kim, S. Park, W. Bosco, R. K. Chidrala and J. Park, *J. Org. Chem.*, 2009, **74**, 2877–2879; (b) W. Cui, Z. Bao,



- M. Jia, W. Ao and H. Zhu, *RSC Adv.*, 2014, **4**, 2601–2604; (c) S. Furukawa, A. Suga and T. Komatsu, *Chem. Commun.*, 2014, **50**, 3277–3280; (d) W. He, L. Wang, C. Sun, K. Wu, S. He, J. Chen, P. Wu and Z. Yu, *Chem.–Eur. J.*, 2011, **17**, 13308–13317; (e) H. Sun, F. Su, J. Ni, Y. Cao, H. He and K. Fan, *Angew. Chem., Int. Ed.*, 2009, **48**, 4390–4393; (f) S. Kegnæs, J. Mielby, U. V. Mentzel, C. H. Christensen and A. Riisager, *Green Chem.*, 2010, **12**, 1437–1441; (g) J. F. Soule, H. Miyamura and S. Kobayashi, *Chem. Commun.*, 2013, **49**, 355–357; (h) L. Zhang, W. Wang, A. Wang, Y. Cui, X. Yang, Y. Huang, X. Liu, W. Liu, J. Son, H. Oji and T. Zhang, *Green Chem.*, 2013, **15**, 2680–2684; (i) C. K. P. Neeli, S. Ganji, V. S. P. Ganjala, S. R. R. Kamaraju and D. R. Burri, *RSC Adv.*, 2014, **4**, 14128–14135; (j) J. W. Kim, J. He, K. Yamaguchi and N. Mizuno, *Chem. Lett.*, 2009, **38**, 920–921.
- 7 (a) M. Langeron and M. B. Fleury, *Angew. Chem.*, 2012, **124**, 1–5; (b) M. Langeron and M. B. Fleury, *Chem.–Eur. J.*, 2015, **21**, 1–7; (c) B. Huang, H. Tian, S. Lin, M. Xie, X. Yu and Q. Xu, *Tetrahedron Lett.*, 2013, **54**, 2861–2864; (d) K. Marui, A. Nomoto, M. Ueshima and A. Ogawa, *Tetrahedron Lett.*, 2015, **56**, 1200–1202; (e) R. D. Patil and S. Adimurthy, *Adv. Synth. Catal.*, 2011, **353**, 1695–1700.
- 8 (a) K. Gopalaiah and A. Saini, *Catal. Lett.*, 2016, **146**, 1648–1654; (b) A. Dhakshinamoorthy, M. Alvaro and H. Garcia, *ChemCatChem*, 2010, **2**, 1438–1443; (c) E. Zhang, H. Tian, S. Xu, X. Yu and Q. Xu, *Org. Lett.*, 2013, **15**, 2704–2707.
- 9 (a) M. Langeron, A. Chiaroni and M.-B. Fleury, *Chem.–Eur. J.*, 2008, **14**, 996–1003; (b) A. E. Wendlandt and S. S. Stahl, *Org. Lett.*, 2012, **14**, 2850–2853.
- 10 (a) X. Lang, H. Ji, C. Chen, W. Ma and J. Zhao, *Angew. Chem., Int. Ed.*, 2011, **50**, 3934–3937; (b) Z. Zhai, X. Guo, G. Jin and X. Guo, *Catal. Sci. Technol.*, 2015, **5**, 4202–4207; (c) D. Ovoshchnikov, B. Donoeva and V. B. Golovko, *ACS Catal.*, 2014, **5**, 34–38; (d) S. Zavahir and H. Zhu, *Molecules*, 2015, **20**, 1941–1954; (e) Y. Li, X. Liu, Z. Yu, Z. Li, S. Yan, G. Chen and Z. Zou, *Dalton Trans.*, 2016, **45**, 12400–12408.
- 11 B. Chen, L. Wang, W. Dai, S. Shang, Y. Lv and S. Gao, *ACS Catal.*, 2015, **5**, 2788–2794.
- 12 (a) W. Liu, L. Zhang, W. Yan, X. Liu, X. Yang, S. Miao, W. Wang, A. Wang and T. Zhang, *Chem. Sci.*, 2016, **7**, 5758–5764; (b) R. V. Jagadeesh, A. E. Surkus, H. Junge, M. M. Pohl, J. Radnik, J. Rabeah, H. Huan, V. Schunemann, A. Bruckner and M. Beller, *Science*, 2013, **342**, 1073–1076; (c) F. A. Westerhaus, R. V. Jagadeesh, G. Wienhofer, M. M. Pohl, J. Radnik, A. E. Surkus, J. Rabeah, K. Junge, H. Junge, M. Nielsen, A. Bruckner and M. Beller, *Nat. Chem.*, 2013, **5**, 537–543; (d) D. Banerjee, R. V. Jagadeesh, K. Junge, M. M. Pohl, J. Radnik, A. Bruckner and M. Beller, *Angew. Chem., Int. Ed.*, 2014, **53**, 4359–4363; (e) L. Zhang, A. Wang, W. Wang, Y. Huang, X. Liu, S. Miao, J. Liu and T. Zhang, *ACS Catal.*, 2015, **5**, 6563–6572.
- 13 (a) J. Long, Y. Zhou and Y. Li, *Chem. Commun.*, 2015, **51**, 2331–2334; (b) Z. Wei, C. Liu, S. Bai and Y. Li, *ACS Catal.*, 2015, **5**, 1850–1856; (c) K. Shen, X. Chen, J. Chen and Y. Li, *ACS Catal.*, 2016, **6**, 5887–5903.
- 14 (a) F. A. Westerhaus, R. V. Jagadeesh, G. Wienhofer, M. M. Pohl, J. Radnik, A. E. Surkus, J. Rabeah, K. Junge and H. Junge, *Nat. Chem.*, 2013, **5**, 537–543; (b) L. Zhang, A. Wang, W. Wang, Y. Huang, X. Liu, S. Miao, J. Liu and T. Zhang, *ACS Catal.*, 2015, **5**, 6563–6572; (c) T. Cheng, H. Yu, F. Peng, H. Wang, B. Zhang and D. Su, *Catal. Sci. Technol.*, 2016, **6**, 1007–1015.
- 15 Z. Wei, J. Wang, S. Mao, D. Su, H. Jin, Y. Wang, F. Xu, H. Li and Y. Wang, *ACS Catal.*, 2015, **5**, 4783–4789.
- 16 K. M. Nam, J. H. Shim, H. Ki, S. I. Choi, G. Lee, J. K. Jang and J. T. Park, *Angew. Chem., Int. Ed.*, 2008, **47**, 9504–9508.
- 17 L. L. Fu, Y. J. Lu, Z. G. Liu and R. L. Zhu, *Chin. J. Catal.*, 2016, **37**, 398–404.
- 18 C. Bai, A. Li, X. Yao, H. Liu and Y. Li, *Green Chem.*, 2016, **18**, 1061–1069.
- 19 W. He, C. Jiang, J. Wang and L. Lu, *Angew. Chem., Int. Ed.*, 2014, **53**, 9503–9507.
- 20 (a) K.-W. Chi, H. Hwang, J. Park and C. Lee, *Synth. Met.*, 2009, **159**, 26–28; (b) J. Long, X. Xie, J. Xu, Q. Gu, L. Chen and X. Wang, *ACS Catal.*, 2012, **2**, 622–631; (c) X. H. Li and M. Antonietti, *Angew. Chem., Int. Ed.*, 2013, **52**, 4572–4576; (d) Y. Gao, G. Hu, J. Zhong, Z. Shi, Y. Zhu, D. Su, J. Wang, X. Bao and D. Ma, *Angew. Chem., Int. Ed.*, 2013, **52**, 2109–2113; (e) H. Wang, X. Zheng, H. Chen, K. Yan, Z. Zhu and S. Yang, *Chem. Commun.*, 2014, **50**, 7517–7520.
- 21 (a) R. D. Patil and S. Adimurthy, *Adv. Synth. Catal.*, 2011, **353**, 1695–1700; (b) Z. Hu and F. M. Kerton, *Org. Biomol. Chem.*, 2012, **10**, 1618–1624; (c) R. D. Patil and S. Adimurthy, *RSC Adv.*, 2012, **2**, 5119–5122; (d) B. Huang, H. Tian, S. Lin, M. Xie, X. Yu and Q. Xu, *Tetrahedron Lett.*, 2013, **54**, 2861–2864; (e) E. Zhang, H. Tian, S. Xu, S. Yu and Q. Xu, *Org. Lett.*, 2013, **15**, 2704–2707; (f) J. Wang, S. Lu, X. Cao and H. Gu, *Chem. Commun.*, 2014, **50**, 5637–5640; (g) S. Zhao, C. Liu, Y. Guo, J. Xiao and Q. Chen, *J. Org. Chem.*, 2014, **79**, 8926–8931.
- 22 F. Su, S. C. Mathew, L. Möhlmann, M. Antonietti, X. Wang and S. Blechert, *Angew. Chem., Int. Ed.*, 2011, **50**, 657–660.

